45

SPATIAL MODELING AND LANDSCAPE CHARACTERIZATION OF AN AFRICAN PASTORAL ECOSYSTEM: A PROTOTYPE MODEL AND ITS POTENTIAL USE FOR MONITORING DROUGHT

MICHAEL B. COUGHENOUR

Natural Resource Ecology Laboratory, Colorado State University, Fort Collins, CO 80523, USA

45.1 INTRODUCTION

Rainfall variation is probably the single most important determinant of changes in ecological condition in sub-Saharan Africa. Ecological indicators for these regions must consider ecosystem responses to rainfall fluctuations that affect plant growth and thus the quantity and spatial distribution of food for livestock and human populations. Much of sub-Saharan Africa is climatically arid to semiarid. Livestock products are the principal source of food for a large number of subsistence pastoralists in these climatic zones and they are an important food source for non-pastoralists as well. The fraction of human nutrition derived from livestock is generally greater in more arid zones. Where rainfall tends to be unpredictable in space and in time, pastoralists tend to be increasingly nomadic.

Over the last decade an interdisciplinary group of scientists have studied the Ngisonyoka subsection of the Turkana tribe of Northwest Kenya (Little *et al.*, 1984; Coughenour *et al.*, 1985; Ellis and Swift, 1988). Turkana nomadic pastoralists occupy the whole northwest portion of Kenya, the Turkana District. Within this region, there are several tribal subsections. Subsectional group members have preemptive grazing rights within the approximate subsectional boundaries. Herdowners in the same subsection are more prone to form alliances and exchange resources during times of food shortage (McCabe, 1987). The Ngisonyoka subsection is located in the southern part of Turkana District (Fig. 45.1).

Droughts are inevitable in Turkana District. The most severe recent drought was in 1979–80. Over 80,000 people occupied famine relief camps in northern and central Turkana by the end of 1980. More recently, the long rains failed in 1984, but it was considered to be a mild drought because rains were good in 1985. The

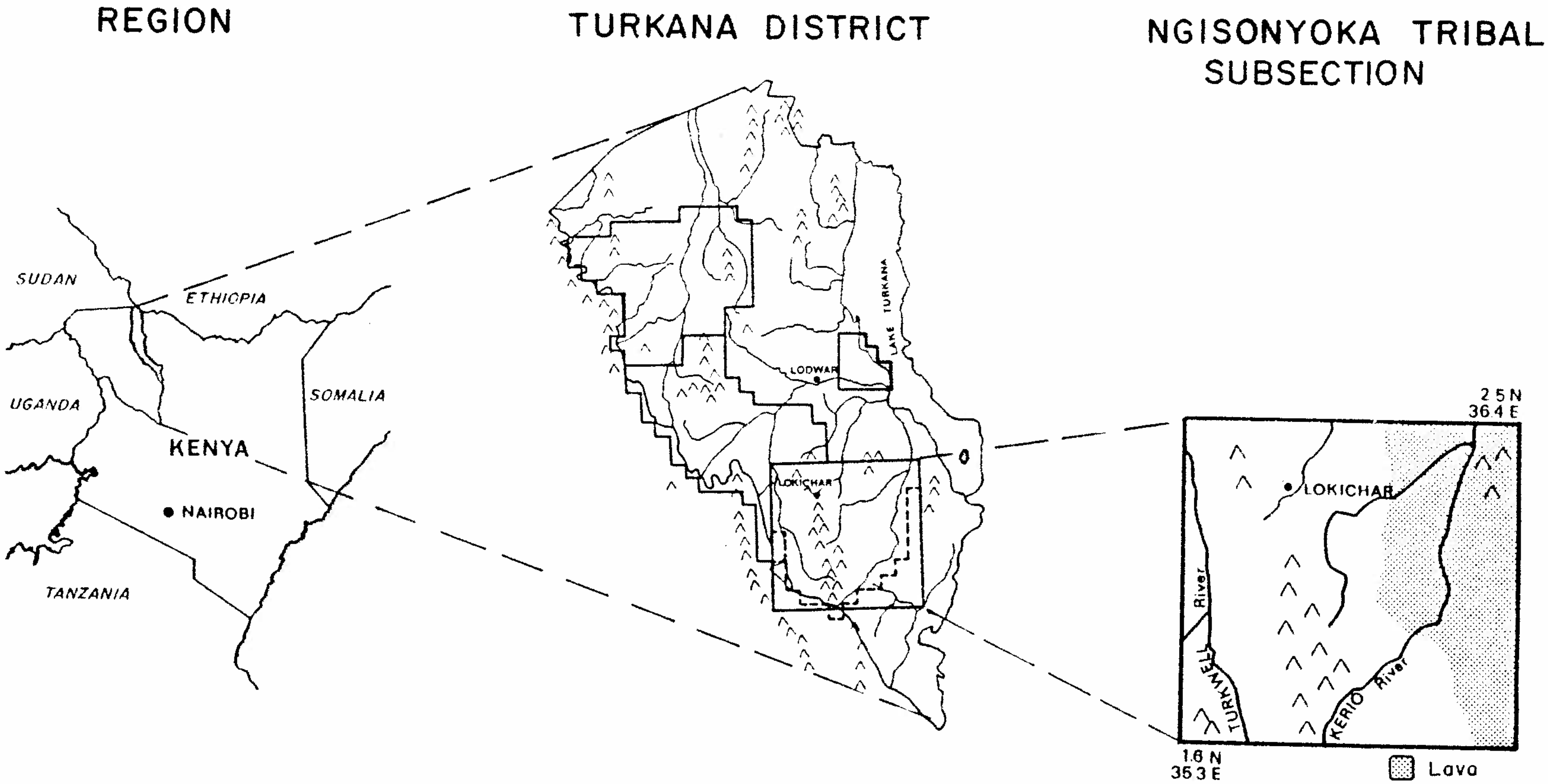

Fig. 45.1. The Ngisonyoka study area location in relation to Turkana District and the region. Shown on the district map are the approximate boundaries around three other tribal subsections (Ellis *et al.*, 1987). The study area encompasses most of the Ngisonyoka subsection, and includes some land that is rarely utilized (beyond the dashed line on the district map). The study area is approximately 125 km east–west by 105 km north–south.

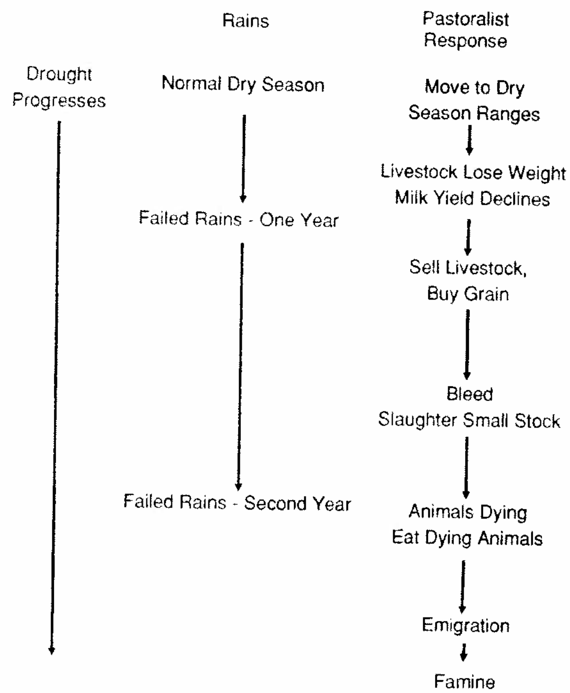

Fig. 45.2. A sequence of events during pastoral drought, leading ultimately to famine if rainfall deficits continue.

Ngisonyoka pastoralists often say that rains will fail on average, one year out of every four. Lodwar weather records indicate that rainfall has dropped below 33% of the mean about once every 3–4 years.

A characteristic sequence of events (Fig. 45.2) occurs as drought progresses (Ellis *et al.*, 1987; Galvin, 1988). First, the rains fail. Second, forage production declines, livestock conditions subsequently deteriorate, and finally human nutrition also declines. During the normal dry season human dietary composition shifts to increased reliance on grains and decreased reliance on milk (Galvin, 1988). During mild droughts, such as in 1984, meat becomes prevalent in the diet as increasing numbers of animals in poor condition are slaughtered. As the rainfall deficit continues, pastoralists must purchase grain by selling off livestock and household items, which results in a decrease in livestock prices during a period of increased grain prices. Famine results as pastoral livestock numbers decrease and as pastoralists are increasingly unable to bridge dietary shortfalls by trading devalued livestock for grain.

McCabe (1983) showed that the Turkana respond to drought by adaptive camp movements and altered land use patterns. Typically, during the wet season pastoralists are most concentrated in a habitat that is easily accessible and has abundant, but transient, forage. As a normal dry season progresses herds are subdivided and the base camp is moved to areas where forage growth is greater but habitat suitability is lower. In Baringo, just south of Turkana, Homewood and Lewis (1987) found three phases of cattle herd management during the mild drought of 1984. The first was a redistribution of livestock to dry season grazing areas. The second was a phase of increased livestock mortality and the third was a period marked by complete absence of calving and a decline of mortality among surviving livestock.

Famine early warning systems (EWS) developed over the last decade have attempted to use knowledge of this chain of events to detect early signs of incipient famine. For example, the main indicator of famine in the EWS developed for Botswana was an increased proportion of children less than five years old weighing less than 80% of the norm for their age (Morgan, 1985). The Botswana EWS recognized that decreased crop growth is an intermediate response to the primary input factor of decreased rainfall. Problems in interpreting the EWS arose from time lags in processing human nutritional data although rainfall data were processed rapidly. This problem suggests that there is a need for more rapid data flow and an increased ability to predict livestock responses to changes in rainfall and declining forage production.

Mason *et al.* (1987) found reports of cattle condition were useful predictors of child nutritional status. Livestock condition indices were formulated to indicate whether livestock were starving, losing weight, maintaining weight, or gaining weight. Cumulative deviations in the livestock index over the normally rainy period of January through April were correlated with child malnutrition reports for July through January.

Swift (1985) designed an EWS for Turkana that considered many different variables including rainfall, range condition, livestock condition, and pastoral movements. His system also emphasized unusual declines in livestock prices associated with increased volume of livestock sales. Eldridge *et al.* (1986) described an EWS for Sudan with many of the same features.

To predict the chain of events between decreased rainfall and the response of human nutritional stress, a process-oriented understanding of the pastoral ecosystem is necessary. Studies have also suggested that pastoral ecology must be studied at a landscape level of organization. Studies conducted on small intensive sites must be transformed to account for system dynamics over a much larger area. Verstappen (1979) suggested that ecological monitoring of entire landscapes was needed to effectively monitor ecosystem response to drought. He suggested combining knowledge of spatial distributions of soil texture, soil water holding capacity, drought resistant vegetation, and topographic effects on water flow with data from ground-, aircraft-, and satellite-based studies. Spatial variations in landscape properties must be integrated with ecosystem processes to understand or predict the dynamics of entire pastoral ecosystems.

A spatial ecosystem model of the Ngisonyoka pastoral ecosystem is described here (first presented in Coughenour, 1989). The model predicts plant responses to rainfall, soils, and topography. Distributions of pastoral livestock population numbers and spatial distributions are simulated based upon forage and habitat resource distributions. National Oceanic and Atmospheric Administration satellite normalized difference vegetation indices imagery are used to analyze and verify predicted vegetation dynamics. The model traces patterns of forage production and livestock foraging to derive a time-varying index of livestock condition for the system as a whole. This index can be viewed as an ecological indicator of drought. A system is proposed that would integrate landscape modeling with rainfall and satellite data on a timely basis to monitor ecological condition and assess the risk of continued drought or famine.

45.2 METHODS

45.2.1 Study area

The Ngisonyoka area is situated entirely within the low-lying Rift Valley (Fig. 45.1), that has elevations ranging from 500 m to 2000 m. A Pre-Cambrian basement-complex mountain range bisects the area. A sandy bajada covers the area immediately east of the central mountain range. Areas west and north of the mountains are a mosaic of sandy alluvial plains, weathered stone mantle soils, and rocky outcrops. Much of the eastern half of the area is covered with highly weathered Miocene lava plains and hills.

Both arid (300–550 mm/year rainfall) and very arid (150–350 mm) ecoclimatic zones are found within the area, with small pockets of subhumid climate at very high elevations. More mesic zones are generally found in the southwest. Mean rainfall at weather stations in the area varies from 201–394 mm/year while potential evapotranspiration is 2200–2700 mm/year. Rainfall is highly seasonal. A period of long rains usually occurs in March–May, while short rains occur around November.

Vegetation in the arid zones is primarily dry thorn bushland, while the very arid zones are mostly dwarf shrub grassland. Most grasses in areas receiving less than 350 mm/year are annual, with an increasing prevalence of perennial grasses in more mesic areas. The area is 10%–40% covered by woody vegetation, mostly *Acacia* spp. and *Commiphora* spp. trees and shrubs.

45.2.2 Spatial model framework

To consider interactions of spatial resource distributions with ecosystem processes, a linkage between spatial data and a simulation model was formed. Linkage between a spatial data base and a simulation model may be achieved by at least three different methods. One of these is to use built-in capabilities of a geographic information system (GIS) for modeling. If the GIS software allows iterated calculations the GIS can be used to simulate change over time. Some GIS systems allow user-supplied subroutines. A second approach is to program a dynamic link between separate GIS and simulation model programs via the computer's operating system. The GIS and simulation model then exchange information over the course of a simulation, but not necessarily at every model time step. The third approach is to incorporate a simple spatial data structure into the model, which is easily achieved by storing model data in two dimensional arrays. The advantage

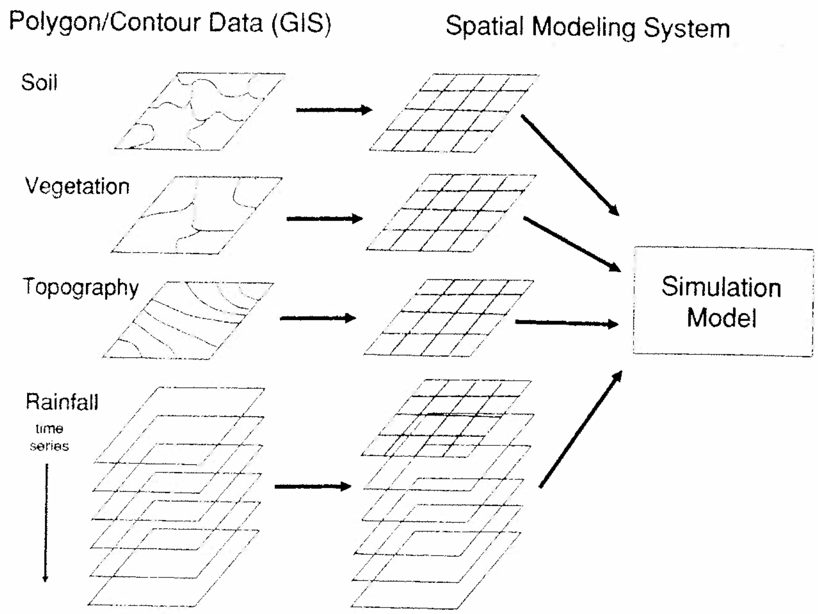

Fig. 45.3. A schematic of the relationship between spatial data stored in geographic information systems (GIS) and the spatial modeling system. Polygon and contour data are converted to a common grid cell data structure for use in the spatial simulation model.

of the third approach is that considerable computational overhead (that associated with running a separate GIS and that arising from information exchange between model and GIS) is eliminated; therefore, it was the approach selected for this study (Fig. 45.3).

The Ngisonyoka tribal subsection was represented as a grid of 5 × 5 km cells. The entire grid was 21 rows by 25 columns, or 13,125 km^2. However, the simulation model only performed calculations for a systematic 50% subsample of these cells in any given run, effectively using a 11 × 13 grid of 143 non-contiguous cells. (See Fig. 45.3.)

Geographic data were converted into a simple raster form for use in the spatial modeling system. GIS data were stored in several different forms. The geographic distribution of soils was mapped as polygons. Polygon data stored in the polygon-based ARC/INFO system were converted to the grid using the POLYGRID command. Soils data were used primarily for computation of water-holding capacity. An aerial survey of woody canopy cover and dwarf shrub cover was conducted (Ecosystems Ltd., 1985) along flight lines corresponding to 10 × 10 km grid cells. These canopy cover data were then converted to the 5 × 5 km grid using spatial interpolation (squared inverse distance weighting). Topographic data were digitized as contours, the GIS converted these data to a high resolution grid which was then converted to the coarse 5 × 5 km modeling grid.

45.2.3 Temporal rain map generation

The spatial distribution of rainfall is needed to predict the spatial distribution of plant growth. Unfortunately, temporal sequences of rainfall maps are often difficult to obtain. Therefore, a method was devised to generate a temporal sequence of rainfall maps from rainfall data gathered at irregularly spaced weather stations in the study area. The sampling method accounted for regional variation as well as elevational effect.

For each month, rainfall data from the known weather stations were entered along with their latitudes, longitudes, and elevations. Regression equations of rainfall on elevation were performed for each month, specifying the 5 × 5 km model grid of x–y coordinates. Elevation for each of these grid points was specified, based on digital elevation data. For each grid point, the four nearest weather stations were located and the distances (D_{ij}) to these stations were computed. Rainfall data for each of these four stations were used to estimate rainfall at the unknown grid point, based on the difference in elevation between the two points and the observed increase in rainfall with elevation. Thus, for the ith known rainfall datum ($i = 1, 2, 3$, or 4) and the jth unknown grid point,

$$\mathrm{ppte}_{ij} = \mathrm{ppt}_i + B\,(\mathrm{E}_j - \mathrm{E}_i)$$

where ppt_i was a known rainfall amount, E was elevation, B was the slope of the rainfall vs. elevation regression equation, and ppte_{ij} was the rainfall estimate. Each of the four estimates (ppte_{ij}, $i = 1, 2, 3$, or 4) was weighted by the fourth power of the inverse distance ($1/D_{ij}^4$) to derive an estimate for the jth unknown point. If the rainfall vs. elevation regression produced a low correlation coefficient, elevation was not used and interpolation was based only on the inverse distance interpolation.

45.2.4 A simple ecosystem model

45.2.4.1 Allocation of rainfall and plant growth

Each month, rainfall and storm number (rainy days per month) estimates were read into the model for each grid cell. A simplified rainfall generator was used to add stochastic variation among days within the month. Rainy days were determined within each month by random sampling from a uniform distribution. It was assumed that the probability of a rainy day equaled the proportion of rainy days observed in the month. For each rainy day, rainfall amount was estimated by random sampling from a gamma distribution using the mean monthly storm size. Randomness was imposed on each grid cell independently of others, which also created spatial patchiness. More elaborate rainfall generators use Markov methods to estimate rainy days and sample from a gamma distribution to estimate rain amount (e.g. Bruhn *et al.*, 1980; Larsen and Pense, 1981).

On a rainy day, rainfall was infiltrated into the soil according to a simple "tipping bucket" model. The top layer was filled to field capacity, and the excess was drained to the subsoil. If the subsoil was saturated, the excess was drained from the system. Evaporation from the topsoil was estimated from potential evapotranspiration and soil moisture content. Evaporation rate was reduced below a maximal rate (7·4 mm/d) as the topsoil dried out.

A highly simplified model of plant growth was formulated to dynamically estimate live and dead forage standing crops. The model simulated production of biomass, transfer of live biomass to standing dead biomass, and transfer of standing dead biomass to soil. Three functionally distinct types of plants were simulated: grasses, dwarf shrubs, and shrubs and trees were distinguished based upon differences in their rooting depths and access to soil water.

It was assumed that a soil moisture content of 50% of field capacity was required for (mainly annual) grass growth initiation at the beginning of a wet season, while 30% soil moisture was needed for perennial shrubs and trees. After the growth initiation phase, maximum growth rates of 10, 4, and $5\,g{*}m^{-2}{*}d^{-1}$ for grasses, dwarf shrubs, and tree/shrub were used to estimate maximum water demands for each type of plant (estimates based on Coughenour *et al.* (1990 *a*, *b*, *c*). Total water demands were estimated by dividing the maximum growth rate by water use efficiency. Water use efficiencies (WUE) were taken as $1{\cdot}3\,g{*}m^{-2}{*}mm^{-1}$ for grass and $0{\cdot}65\,g{*}m^{-2}{*}mm^{-1}$ for shrubs and trees. The value for grass was estimated so that model predictions matched observed rain use efficiencies (Coughenour *et al.*, (1990*b*). A two-fold difference in WUE between C4 grasses and C3 shrubs and trees was based on relative differences in WUE commonly observed between these groups (e.g. Fischer and Turner, 1978).

The total water demands of the three plant groups were summed. Demands were partitioned among soil layers according to specified rooting distributions. Grasses were assumed to root exclusively in the top soil, dwarf shrubs to root equally in top soil and sub-soil, and tree/shrubs were assumed to have 70% of their roots in sub-soil. If the water demands in a layer exceeded the soil supply, then the actual water use by each plant group was estimated by allocating the available water among the plant groups in proportion to their demands. Plant growth (from a soil water layer) was reduced accordingly. The realized water use for each type was multiplied by its WUE to arrive at actual above ground plant growth (from a soil water layer).

The death of green tissues, and concomitant transfer to standing dead biomass, was determined as the product of a maximum rate, a function of soil moisture in a soil water layer, and the standing green biomass. Maximum rates were 0·05, 0·03, and $0{\cdot}01\,d^{-1}$ for grass, dwarf shrubs, and tree/shrub respectively. The parameters for the soil moisture effect were determined such that mortality at wilting point occurred at the maximum rate while no mortality occurred at field capacity. The proportion of total biomass dying due to dry soil in a given layer was proportional to the fraction of roots found in that layer. Standing dead biomass was transferred to soil litter (including abiotic weathering and termites) at a rate of 20% per day. Litter decomposition was not simulated.

45.2.4.2 Livestock spatial distributions, forage consumption and condition

Pastoral livestock distribution was modeled at the population-level, rather than the individual-level. The entire population was redistributed in relation to habitat and forage resources. This approach stands in contrast to a model of the movements of individual animals in a pasture (Pickup and Chewings, 1988). An individual based modeling approach over regional areas, would be highly demanding of computer resources, as it would require modeling the activities of a very large number of pastoralists responding to local environments. Furthermore, it would necessitate modeling interactions among individual herdowners as they compete for, or allocate, available resources. A drawback of the population-level (aggregate) approach is that costs of movement must be assumed to be randomly distributed through the population. A map representing danger from raiding neighboring tribesmen could optionally be used to limit pastoral distributions.

The total number of livestock in the simulated Ngisonyoka ecosystem, based on population estimates and human/livestock ratios (Ecosystems Ltd., 1985) was 20,000 head, including sheep, goats, cattle, camels, and donkeys. Other inputs to the model included a map of the preferred wet season range, and a map showing locations of water sources (temporary and permanent wells). The water source map was used to calculate distance to water for each grid cell.

A new livestock distribution was calculated every twelve days. This interval was similar to a maximal movement frequency of about 10–15 days (McCabe, 1983). At each interval, the average standing green grass biomass was calculated on the wet season range. If the wet season range standing crop was greater than a specified value ($20\,g/m^{-2}$), then livestock were distributed over the wet season range in proportion to the distribution of grass standing crop. When simulated pastoralists were using their wet season range, a maximum of 100 head/km^2 were allowed if there was $100\,g/m^2$ of live grass biomass while the maximum stocking rate declined to 25 head/km^2 at $45\,g/m^2$ grass biomass. If a proportion of the population could not be allocated into the wet season range given this constraint, then that remainder was distributed in accordance with the dry season range allocation rules below.

When there was insufficient biomass on the wet season range to allow population concentration there, the following rules were invoked to simulate the population distribution over the total ecosystem area. Populations were distributed in proportion to a habitat value index or weighting factor. This weighting factor was calculated as the product of a forage value factor and the minimum of constraints due to slope, woody cover, elevation, distance to water, and proximity to raiding tribesmen. The forage value factor was proportional to forage biomass, up to a maximal value at $100\,g/m^2$. Grid cells having average slopes in excess of 8% were considered unusable. Woody canopy cover was assumed to be optimal at 25%. Habitat suitability declined at rates below 25% because of insufficient shade, and the habitat declined at rates above the 25% canopy cover due to physical inaccessibility (thickets). Grid cells with elevations of 550–900 m were ranked with a higher value than were lower elevations, which are infrequently used due to excessive temperatures and scarce water, and higher elevations, which are disfavored due to lack of water and difficult terrain. Grid cells that were more than 25 km from water were not used, whereas cells that were within 5 km of water were most preferred.

Forage intake rate was modeled with a functional response curve, where forage intake rate increased in relation to food abundance. The consumption rate of each forage type in a grid cell was calculated and the distribution of total foraging time among plant groups was set proportional to these rates. The maximal total rate of green forage intake was calculated as 4 kg*head^{-1}*d^{-1} and the maximum forage intake rate of dead forage was set at 2 kg*head^{-1}*d^{-1}, reflecting the fact that ruminant digestion rates are slower when forage quality is lower.

An animal condition index was calculated to integrate cumulative forage intake relative to forage requirement. The condition index increased in proportion to forage intake in excess of nominal requirements. When forage intake rate was below the minimal forage requirement livestock conditions decreased. The change in condition index at each time step equaled the difference between kg/d forage intake and kg/d forage requirement. Thus, if intake was below requirements the index declined, which might be indicative that livestock would be losing weight. The converse was true if intake was above requirements. Condition index was bounded between −150 kg and 150 kg forage equivalents. The nominal requirement of 2 kg*head^{-1}*d^{-1} was derived from average animal size in the herd, and a requirement of 2·5% of body weight per day. Swift (1987) and Hearne and Buchan (1990) modeled changes in animal condition indices differently, and used the indices to influence simulated rates of livestock weight gain or loss, milk production, reproduction, and mortality.

45.2.5 Model comparison to satellite data

Normalized difference vegetation indices (NDVI) were derived from reflectance data from the advanced very high resolution radiometers (AVHRR) on board NOAA polar orbiting satellites (Tucker *et al.*, 1983, 1985; Prince and Tucker, 1986). NDVI has been shown to be correlated with green leaf biomass. These NDVI data were especially useful for verifying the temporal and spatial variations in model predictions of biomass. Comparisons of model predictions to NDVI were not, however, validations of the model or the NDVI, because the NDVI is an indirect measure of plant biomass. The NDVI has not been fully calibrated against direct field measurements in our study area.

The data set provided by the National Aeronautics and Space Administration (NASA) Goddard Space Flight Center was a monthly series of windowed NDVI images for northern Kenya. Pixel size was approximately 7·5 × 7·5 km. The data had been radiometrically calibrated and registered. The images were further windowed for the Ngisonyoka study area. The raster was then spatially interpolated (inverse distance weighting) to 5 × 5 km resolution to facilitate comparison with the 5 × 5 km model grid.

Comparisons of model output against NDVI were conducted in both the spatial and the temporal domains. Percentages of observed variance explained by the model were calculated by calculating the linear correlation coefficient (r) between model predictions and observed data. These comparisons were performed to measure goodness of fit rather than to statistically estimate model validity. Thus, probability or significance levels are not reported. Autocorrelation in the spatial domain violated the assumption of sample independence that is required for significance testing.

In the spatial domain, sums of squared deviations were calculated each month

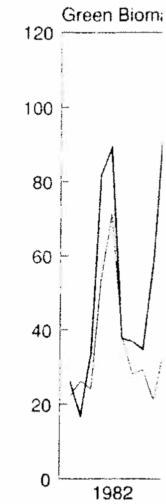

Fig. 45.4. Comparison
satellite derived normal

for variations in the
NDVI among 143 g
squares explained by
In the temporal do
on the sum of values
Twenty such 15 km
culated for each mon
The percentage sums
were averaged each y
of fit for the year. M
objectively, in contra
over time.

The model was simul
forage biomass comp
over the entire stud
generally coincident
showed their greatest
the model and the
fluctuations in NDV
simulated small peal
Greatest discrepanci

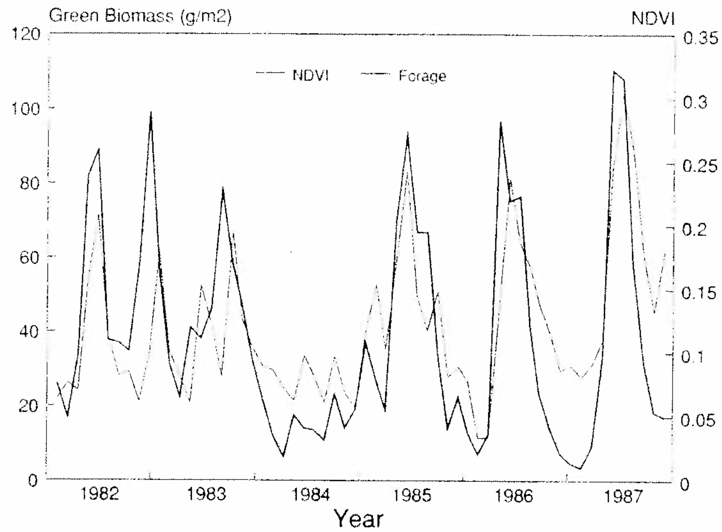

Fig. 45.4. Comparison of simulated dynamics of total standing crop of green biomass with satellite derived normalized vegetation index (NDVI). Both measures are averaged over all 5×5 km grid cells in the study area.

for variations in the model prediction of total standing green biomass and the NDVI among 143 grid cells. The twelve monthly values for percentage sums of squares explained by the model were averaged each year.

In the temporal domain, NDVI and model predictions comparisons were based on the sum of values in a neighborhood of three closest grid cells to the study grid. Twenty such 15 km^2 areas were analyzed. Sums of squared deviations were calculated for each month over a twelve month period for each neighborhood group. The percentage sums of squares explained by the model for each neighborhood were averaged each year among neighborhoods to give a single index of goodness of fit for the year. Model performance could be assessed relatively quickly and objectively, in contrast to visual comparisons of NDVI and model output images over time.

45.3 MODEL RESULTS

The model was simulated over the period of 1981–1987. Modeled dynamics of total forage biomass compared favorably with observed fluctuations in NDVI, averaged over the entire study area (Fig. 45.4). Time of peak simulated biomass was generally coincident with time of peak NDVI. Both the model and the NDVI showed their greatest values in the last year (1987), while minimal values for both the model and the NDVI occurred in the third year (1984). Several smaller fluctuations in NDVI were also simulated by the model. For example, the model simulated small peaks both before and after the main peak in the third year. Greatest discrepancies between model and NDVI were in the minimal values

Table 45.1
Percentage of sums of squares of NDVI about its mean that can be explained by model predicted variation in standing green biomass. The spatial domain represents variation among grid cells in the region, while the temporal domain includes variation among months in a year for individual grid cells

Year	*Percentage of variance*	
	Spatial	*Temporal*
1982	60	55
1983	47	23
1984	36	15
1985	46	26
1986	37	61
1987	49	71

between peaks, and in the rate and timing of biomass decline. The model tended to predict earlier declines than those detected by the NDVI and model predictions often declined to relatively lower minima.

Correlations between modeled total green biomass and NDVI varied in strength among years (Table 45.1). Spatial correlations were generally better than temporal correlations. As would be expected, both spatial and temporal correlations were weaker in drier years. The poorest relationships were noted in 1984, the year the long rains failed.

The dynamics of rainfall, forage biomass, and animal condition are shown in Fig. 45.5. Forage biomass dynamics generally lagged one or two months behind precipitation fluctuations, as a consequence of soil water storage and its subsequent use for plant growth. Both large and small peaks in forage standing crops could be explained by preceding months of favorable rainfall.

The simulated animal condition index exhibited fluctuations that reflected foraging conditions over longer antecedent time periods (Fig. 45.5). The condition index usually declined during dry seasons. The condition index declined to much lower levels in longer dry seasons. During 1982 the index indicated gradual recovery from a low state induced by the drought of 1980–81. The year 1983 was not particularly wet, but animal condition was sustained throughout the normally dry period due to intermittent rains. Heavy rains late in 1983 pushed the index to a higher level. The longest period of low animal condition occurred during the drought year of 1984. Good rains in 1985 and 1986 pushed the index to high levels.

Spatial distributions of rainfall, forage biomass, and NDVI were very similar (Fig. 45.6), reflecting the regional rainfall pattern (Fig. 45.6(a)). Generally the highest values occurred in the southwest, with values declining towards the northeast of the region. Spatial variations in rainfall (Fig. 45.6(a)), forage (Fig. 45.6(b)), and NDVI (Fig. 45.6(c)) strongly reflected topography of the area, since the highest

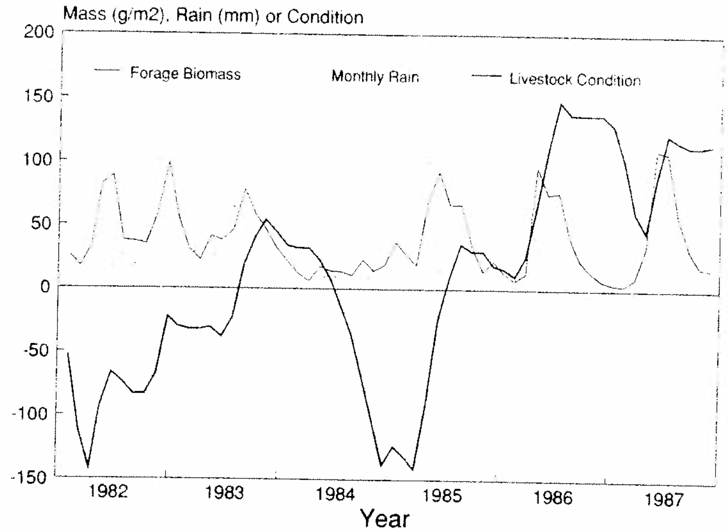

Fig. 45.5. Temporal dynamics of monthly rainfall, total standing crop of green forage, and the animal condition index for the years 1982–1987. Units of the condition index are kg forage equivalents per animal.

elevations were in the southwest. High rainfall values were also interpolated over the central mountain range as a direct consequence of elevation data in the spatial interpolation. However, neither simulated forage mass nor NDVI exhibited marked responses to high elevations in the central mountains. The influence of a high elevation area in the extreme northeast could be seen in rainfall, biomass, and NDVI. The relative increase in NDVI with elevation in the northeast was not as large as the increase of rainfall or biomass, suggesting an overemphasis of elevational effect in that area. The driest conditions and lowest forage biomass were in the extreme southeast, which was the area of lowest elevation (Suguta Valley).

Time averages of simulated livestock density distributions (Fig. 45.7) were in general agreement with studies of pastoral movement patterns (McCabe, 1983; McCabe and Ellis, 1987). Highest livestock densities were predicted in the south and southwest parts of the region (Fig. 45.7(a)) due primarily to high forage abundance, but also to flat terrain and availability of water. Moderate livestock densities were predicted for areas in the central part of the region and also in an area towards the east (Fig. 45.7(b)). Much of this area encompasses the wet season range, with moderate forage abundance and good water availability. Local areas of low livestock density within this area corresponded with mountain peaks. Least dense livestock use areas were in areas of extremely mountainous terrain in the central and western parts of the region and in very dry northeast and southeast parts of the region (Fig. 45.7(c)).

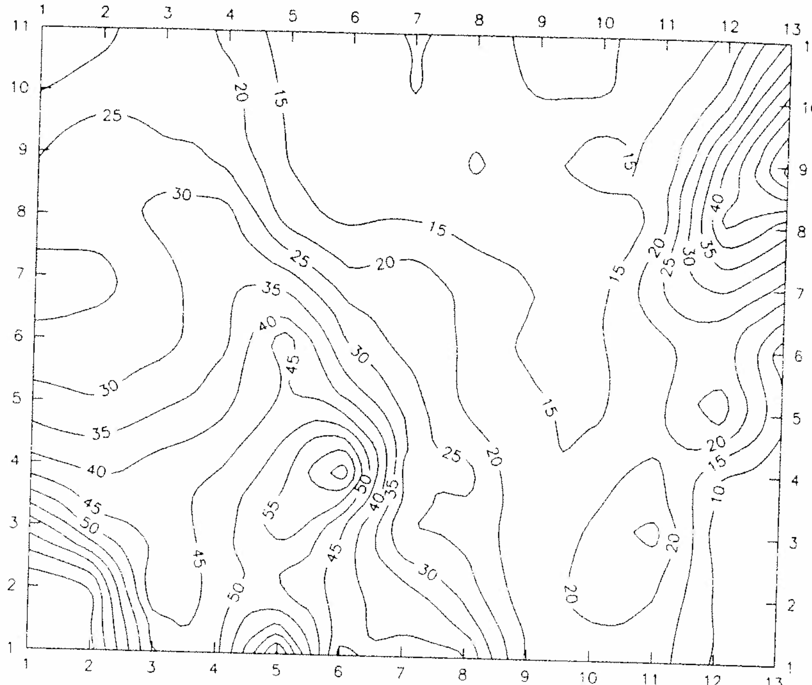

(a)

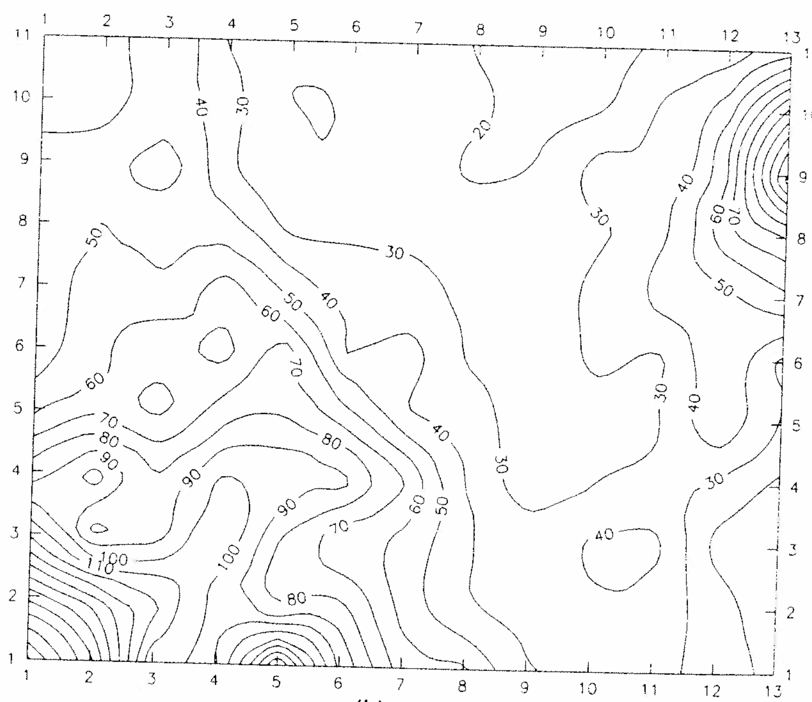

(b)

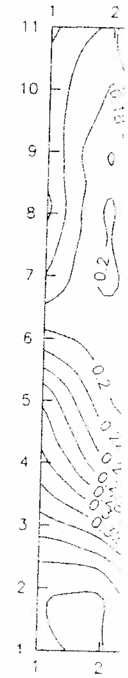

Fig. 45.6. (a) Spa
as predicted by tl
to indices of simı
foliage predicted
index (NDVI) as

45.4

To assess droug
to predict the r
subsequent decli
(Fig. 45.5) and t
decreasing rains
fall at the end of
prior to a declin
two months late
decline in anima
below zero, it wa
of failed rains h
famine.

Decisions for
of levels of rece

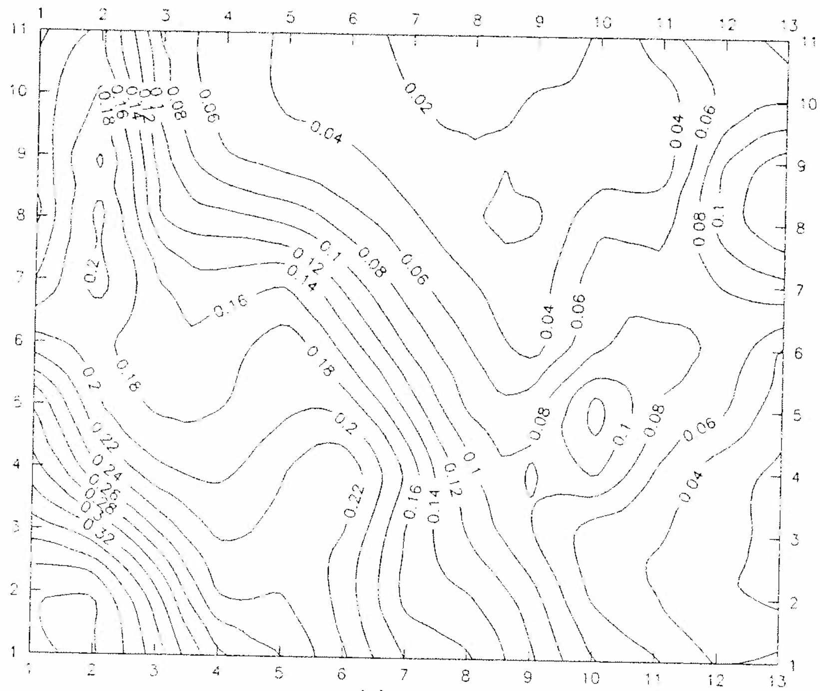

(c)

Fig. 45.6. (a) Spatial distribution of mean monthly rainfall over the study area, 1982–1987, as predicted by the spatial interpolation method described in the text. Units on axes refer to indices of simulated grid cells. (b) Spatial distribution of mean standing crop of green foliage predicted by the model, 1982–1987. (c) The mean normalized difference vegetation index (NDVI) as sensed by NOAA polar orbiting satellites, 1982–1987, over the study area (C.J. Tucker, 1988, pers. comm.).

45.4 MODELING TO ASSESS DROUGHT EFFECTS

To assess drought effects and anticipate subsequent famine it is necessary to be able to predict the negative consequences of low rainfall for forage production and subsequent declines in livestock condition. The model simulated this causal chain (Fig. 45.5) and there were significant time lags in the model between the onset of decreasing rains and following declines in livestock condition. The decline in rainfall at the end of the second simulated year (Fig. 45.5) occurred at least one month prior to a decline in forage. Animal condition did not begin to decline until at least two months later. The continuing lack of rain through the next year led to a large decline in animal condition. When the livestock condition index had dropped well below zero, it was evident that a one year drought was in progress. If a second year of failed rains had occurred there would likely have been a heightened risk of famine.

Decisions for drought intervention are often based upon a relative comparison of levels of recent rainfall with the previous "normal" rainfall levels for that

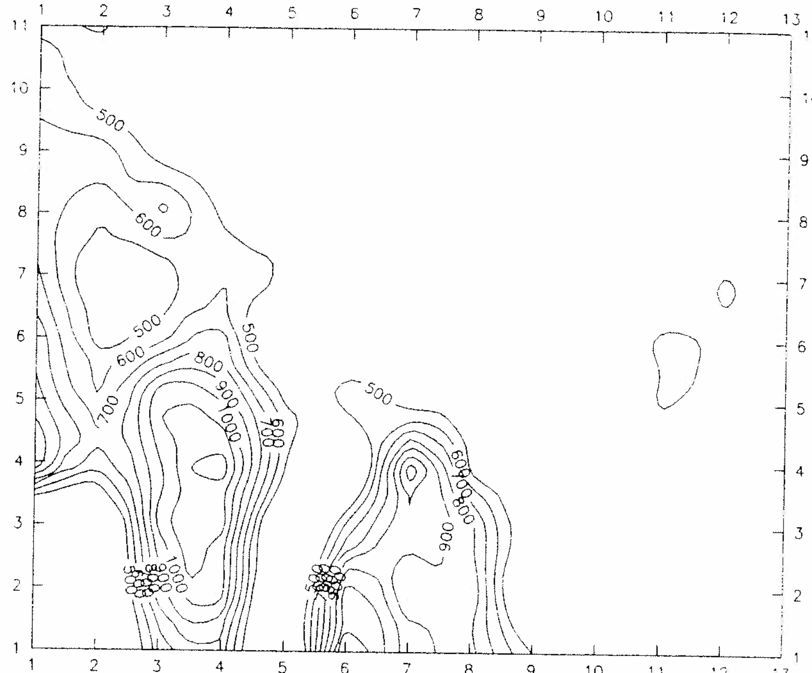

(a)

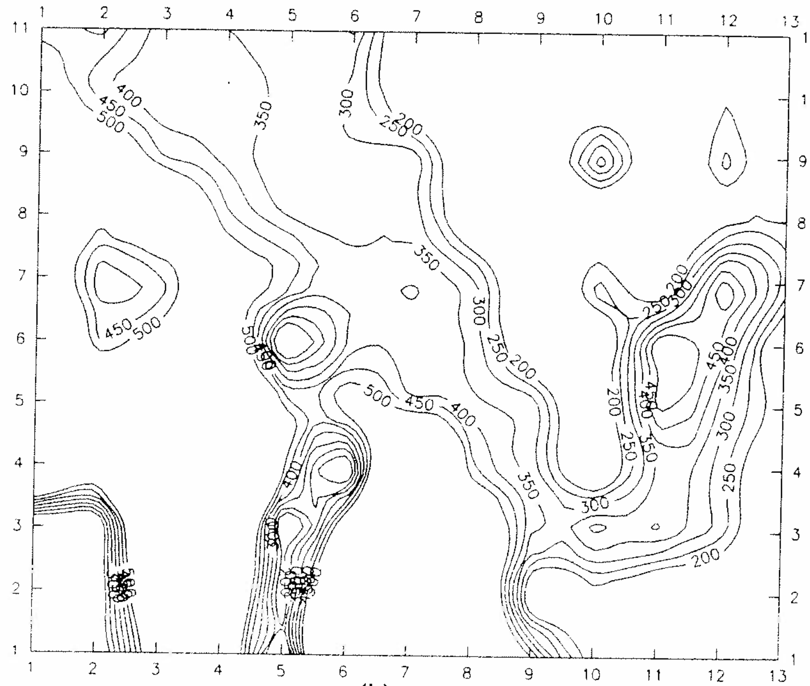

(b)

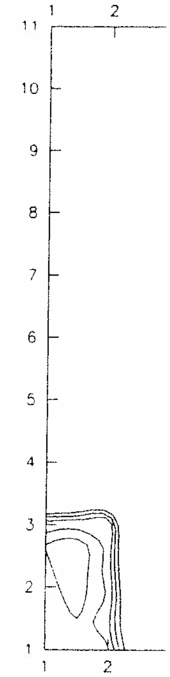

Fig. 45.7. Simulated
livestock per 25 km²
Areas with moderate

location. The seve
level of rainfall d
monitoring systen
system was based
ity distribution of
period of three or
of all prior years.
that which occurre
percentile values
review.

A problem with
dry season month
season months. Al
of rainfall. Classic
November. Howe
also fallen in typic

Use of annual ra
tive probability di

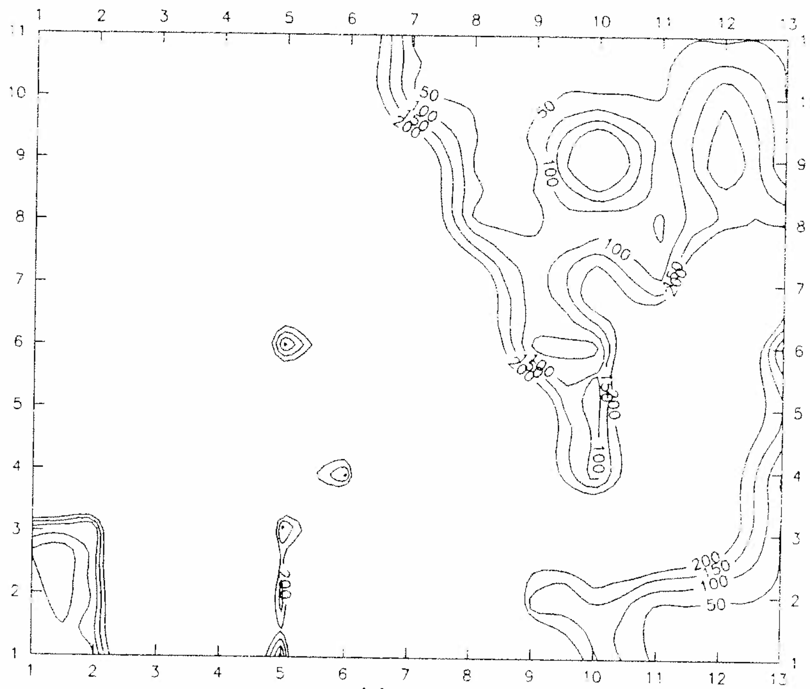

Fig. 45.7. Simulated distributions of livestock averaged over months, 1982–1987. Units are livestock per 25 km^2 grid cell. (a) Areas with highest average densities (500–1200 Head). (b) Areas with moderate densities (200–500 Head). (c) Areas with lowest densities (< 200 Head).

location. The severity of the incipient drought is often ranked in relation to the level of rainfall deficit that has imposed stress in the past. A national drought monitoring system for Australia was described by Lee (1979). The Australian system was based upon comparisons of recent rainfall amounts with the probability distribution of rainfall. In Australia, a serious rain deficiency was defined as a period of three or more months where rainfall was less than that in the driest 10% of all prior years. Drought was designated as severe if recent rainfall was less than that which occurred in the driest 5% of all previous years. Monthly maps of these percentile values were produced and formed the basis of an ongoing drought review.

A problem with applying a three month criterion is that a 10% rainfall level in dry season months will have far less consequence than a similar deficit in wet season months. Also confounding this criterion is the erratic seasonal distribution of rainfall. Classically, the long rains occur in April–May and the short rains in November. However, rains have been known to fail in April–May and rains have also fallen in typically dry months.

Use of annual rainfall probability may circumvent these difficulties. The cumulative probability distribution of annual rainfall in Lodwar, Turkana over a 60 year

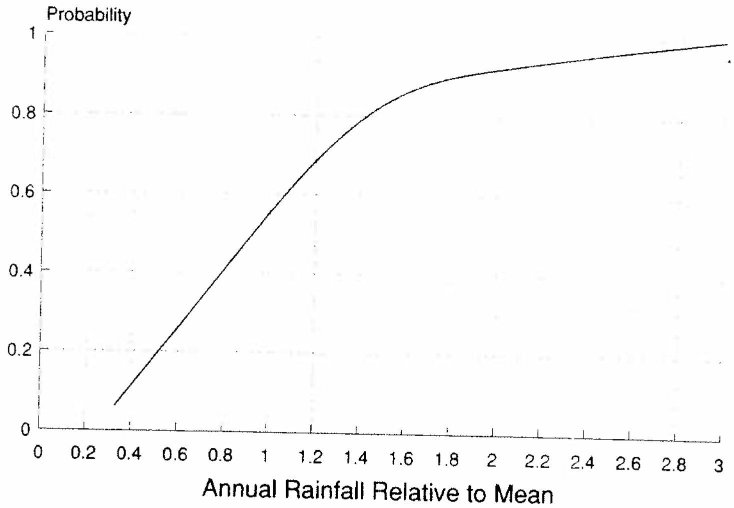

Fig. 45.8. Cumulative probability distribution of annual rainfall observed in Lodware, Turkana relative to the mean, 1929–1989.

period is shown in Fig. 45.8. This distribution indicates, for example, that there is a 20% probability that rainfall over a given year will be less than or equal to about 50% of the long-term mean.

Experiments with the model suggest that livestock condition will decrease substantially between the 66% and the 50% rainfall probability levels (Fig. 45.9). Three years of rainfall at the 66% probability level led to gradually increasing animal condition. However, three years of rainfall at the 50% level caused a decline in animal condition with subsequent persistence of poor condition. Below the 50% level, the recovery periods are even less effective. Knowledge of such outcomes would be useful for assessments of current or incipient drought stress.

While the likelihood of famine depends on current drought stress, the realization of famine depends on the probability of continued low rainfall. Drought risk assessment would be improved if the probabilities of continued rainfall deficit and its consequences were considered. Estimates of future rainfall could be based upon statistics or more sophisticated meteorological modeling procedures. Rainfall predictions would be used by the ecological model to assess ecological consequences.

A statistical approach might consider whether or not annual rainfall was a Markovian process. For example, if the current year was dry, then the probability of the next year being dry might be lower than if the current year was wet. This proved not to be the case in Lodwar. Of the 56% of years when rainfall was below the mean, 62% of the time they were again followed by years with rainfall below the mean. Thirty eight percent of these years were followed by years with rainfall below 66% of the mean. Thus the probability of below average rainfall was not substantially altered by the occurrence of a preceding dry year.

If long range forecasting can improve to the point of allowing predictions of high probability of drought in the next 0–3 years, then that information could be used

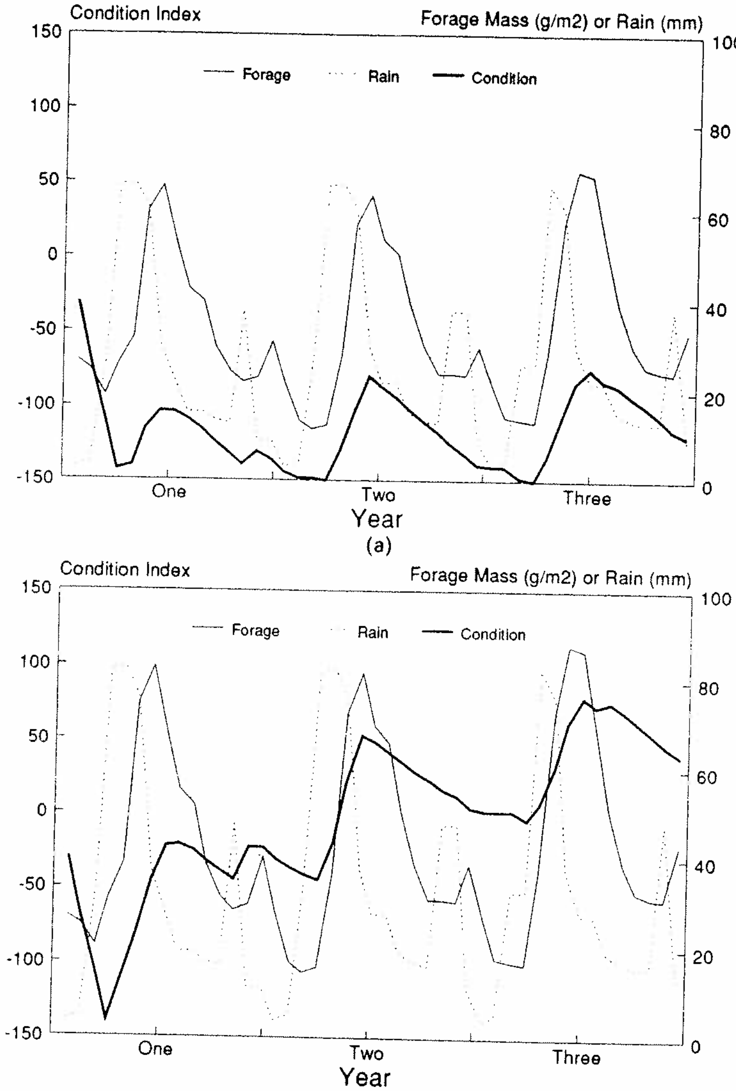

Fig. 45.9. Model simulations of forage and livestock condition responses with rainfall that is (a) 33% and (b) 50% of the long-term mean.

by the model to improve risk assessment. Unfortunately, the prospects for predicting the exact timing of drought are bleak unless rainfall fluctuations have regular periodicity with large amplitude. Even then, rainfall for individual years is not likely to be predictable (Kane and Triverdi, 1986). These authors noted, however, that there was promising ongoing research into teleconnections between terrestrial rainfall patterns and remote sea surface temperatures via ocean-atmosphere interactions.

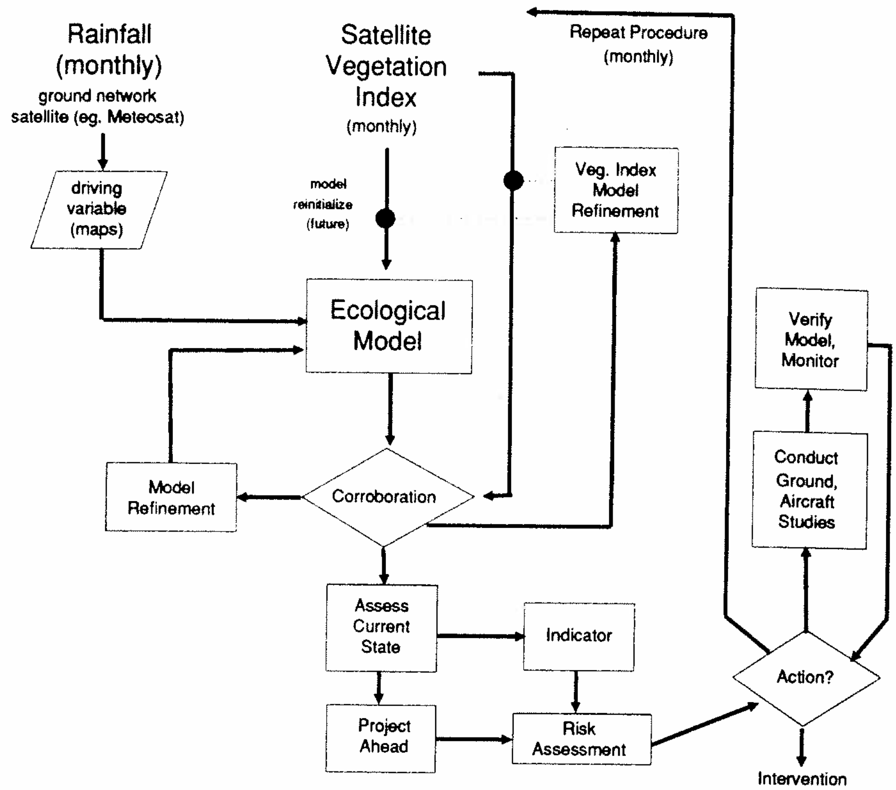

Fig. 45.10. A potential drought monitoring and famine early warning system that integrates rainfall data with an ecosystem model and data from space-borne sensors.

45.5 SYSTEMS APPROACH TO DROUGHT MONITORING

This exercise suggests that a combination of spatial modeling, remote sensing, and rainfall data processing would provide an effective drought monitoring system (Fig. 45.10). In such a monitoring system, monthly rainfall data would be used to drive an ecological model. Rapid processing of rainfall data into maps would increase the effectiveness of this system. Eventually, satellites such as Meteosat may be able to provide mapped rainfall information, as well as soil moisture determinations (Milford, 1987). Satellite NDVI data would be used to corroborate model predictions. Eventually, NDVI data may be used to correct or reinitialize the model. NDVI data would not be the most effective driving variables for this model because NDVI data are time-lagged behind rainfall. If rainfall data are available, these would be more effectively used to anticipate drought. NDVI data are more useful to assess the current state of the system and to corroborate model predictions.

Each month, the model could be used to assess risks of a continuing drought. A model calculation based upon actual rainfall data that are corroborated with

NDVI would be an effective ecological indicator of current system state. This indicator would be used to assess risk, and risk level would be used to decide among alternative actions. Alternatives would include ongoing monitoring and periodic ground and aircraft surveys to verify or correct the model or intervention (e.g. famine relief).

Spatial modeling is needed to calculate the ecological implications of altered rainfall patterns. Rainfall effects on an ecological system are modified by spatial variations in topography, soils, and vegetation. The joint spatial distributions of these variables influences system response. A model is used to integrate these distributions and their significance for ecosystem function.

Modeling increases the utility of satellite data for drought monitoring and assessment. Satellite derived vegetation indices do not directly measure many aspects of the system such as below-ground plant biomass, dead or woody biomass, livestock populations or their condition. Even simple models, which relate satellite indices of green leaf biomass to other ecological variables, may substantially increase the utility and inferential power of these indices (Waring *et al.*, 1986).

Implementation of a spatial modeling and remote sensing scheme over larger areas will require a larger network of information flow. Monitoring over larger regions can be achieved through a hierarchically organized system where information flows upwards from local studies to provide assessments over larger spatial areas. Ellis *et al.* (1987), for example, studied four subsections in Turkana District to understand district-wide drought response patterns. District-level information can in turn be integrated to assess drought at national or multi-national levels.

Local studies should be performed over spatial areas similar in size to the Ngisonyoka area to obtain in-depth understanding of system responses (see also Homewood and Lewis, 1987). Pastoralists respond to seasonal and yearly rainfall variations by moving over the Ngisonyoka subtribal spatial scale. The ability of pastoralists to withstand drought cannot be determined unless the effects of their movements are taken into account. Nomadic pastoralists effectively integrate heterogeneous and variable resource distributions through their complex behavioral and ecological interactions with the landscape.

45.6 CONCLUSIONS

Famine early warning systems or drought monitoring systems have often been limited by two factors. Some systems have been based on measurements of drought responses such as changes in livestock markets or human nutrition. Such a limitation can be overcome by considering rainfall, the lack of which is the essence of drought. To use rainfall variation as an early warning, the ecological consequences of rainfall for pastoralists must be predicted. Thus, the second limitation of some monitoring systems is that the implications of altered rainfall patterns cannot be clearly defined.

A procedure that predicts livestock condition and subsequent pastoralist nutritional responses to rainfall would achieve this end. The most important intermediate variable is forage abundance and distribution. A system that includes rapid verification of predicted forage abundance and distribution would be preferred. A workable methodology may include simulation modeling of ecological responses over sub-regional land areas.

A systematic approach is needed to overcome these limitations. Simulated livestock condition appears to be a promising index for assessing susceptibility to famine when it is calculated in the context of a spatial ecological simulation model. In the model presented here it was demonstrated that even a simple simulation model can work through a set of calculations that account for effects of livestock movements, spatial forage distributions, and other variables. Simulated changes in the simulated livestock index reflected cumulative changes in rainfall, forage growth, and grazing activities, effectively integrating spatial and temporal variability while accounting for effects of pastoral strategies. Satellite and ground-based information are required to verify and update the model over the short term and to improve the model over the long term. Over time, understanding of drought prone ecosystems would improve, along with the ability to monitor drought and prepare for its effects.

ACKNOWLEDGEMENTS

Research was supported by NSF grant DEB-8004182. J. G. Wyant initially suggested that this model be applied as an ecological indicator of drought in Africa. Spatial modeling of this pastoral system has benefitted greatly from discussions with J. E. Ellis and D. M. Swift. C. J. Tucker provided an essential NDVI data set. J. T. Hart provided early ideas for use of GIS and remote sensing.

REFERENCES

Bruhn, J. A., W. E. Fry and G. W. Fick (1980). Simulation of daily weather data using probability distributions. *J. Appl. Meteorl.*, **19**, 1029–36.

Coughenour, M. B. (1989). Ecosystem processes integrated by nomadic pastoralists. Paper presented at the Fourth Annual Landscape Ecology Symposium, International Association for Landscape Ecology, Ft Collins, CO.

Coughenour, M. B., J. E. Ellis, D. M. Swift, D. L. Coppock, K. Galvin, J. T. McCabe and J. T. Hart. (1985). Energy extraction and use in a nomadic pastoral ecosystem. *Science*, **230**, 619–25.

Coughenour, M. B., D. L. Coppock, M. Rowland and J. E. Ellis. (1990*a*). Dwarf shrub ecology in Kenya's arid zone: *Indigofera spinosa* as a key forage resource. *J. Arid Environ.*, **18**, 301–12.

Coughenour, M. B., D. L. Coppock, and J. E. Ellis. (1990*b*). Herbaceous forage variability in an arid pastoral region of Kenya: importance of topographic and rainfall gradients. *J. Arid Environ.*, **19**, 147–59.

Coughenour, M. B., J. K. Detling, I. E. Bamberg and M. M. Mugambi. (1990*c*). Production and nitrogen responses of the African dwarf shrub *Indigofera spinosa* to defoliation and water limitation. *Oecol.*, **83**, 546–52.

Ecosystems Ltd. (1985). Turkana District Resources Survey 1982–1984. Main Report,

Ministry of Energy
Republic of Kenya
Eldridge, El, C. Salte
Sudan. *Disasters*,
Ellis J. E. and D. M
paradigms and im
Ellis, J. E., K. A. Ga
in Turkana Distri
Development (NO
Hearne, J. W. and A
management polici
Agric. Systems, **33**,
Homewood, K. and
Kenya 1983–85. *J.*
Fischer, R. A. and N.
Rev. Plant Physiol.
Galvin, K. A. (1988).
12, 147–56.
Kane, R. P. and N. B
Larsen, G. A. and R.
Dept. Agric., Stat.
Lee, D. M. (1979). A
Drought in Botswa
New England.
Little, M. A., N. Dys
Human biology and
in anthropology, ed.
Mason, J. B., J. G. H
Using agricultural
nutrition on Botsw
McCabe, J. T. (1983
109–126.
McCabe, J. T. (1987).
tion. *J. Res. Econ.*
McCabe, J. T. and J. E
33–41.
Milford, J. R. (1987).
Meteosat data. *Soil*
Morgan, R. (1985). T
in Botswana. *Disas*
Pickup, G. and V. H.
of cattle movement
Prince, S. D. and C. J.
II. NOAA AVHRR
Swift, D. M. (1987). St
in Turkana District
A report to the Nor
Kenya.
Swift, J. (1985). Planni
and Turkana Rehab
Tucker, C. J., C. VanP
of total dry matter
Tucker, D. J., J. R. To
satellite data. *Scienc*

Ministry of Energy and Regional Development and the Turkana Rehabilitation Project, Republic of Kenya, Nairobi.
Eldridge, El, C. Salter and D. Rydjeski. (1986). Towards a famine early warning system in Sudan. *Disasters*, **10**, 189–96.
Ellis J. E. and D. M. Swift. (1988). Stability of African pastoral ecosystems: Alternate paradigms and implications for development. *J. Range Manage.*, **41**, 450–9.
Ellis, J. E., K. A. Galvin, J. T. McCabe and D. M. Swift. (1987). Pastoralism and drought in Turkana District, Kenya. A report to the Norwegian Agency for International Development (NORAD), Nairobi, Kenya.
Hearne, J. W. and A. J. C. Buchan. (1990). A model to analyse the influence of resource management policies on the economic returns from a traditional African pastoral system. *Agric. Systems*, **33**, 77–96.
Homewood, K. and J. Lewis. (1987). Impact of drought on pastoral livestock in Baringo, Kenya 1983–85. *J. Appl. Ecol.*, **24**, 615–31.
Fischer, R. A. and N. C. Turner. (1978). Plant productivity in arid and semiarid zones. *Ann. Rev. Plant Physiol.*, **29**, 277–317.
Galvin, K. A. (1988). Nutritional status as an indicator of impending food stress. *Disasters*, **12**, 147–56.
Kane, R. P. and N. B. Triverdi. (1986). Are droughts predictable? *Clim. Change*, **8**, 209–23.
Larsen, G. A. and R. B. Pense. (1981). Stochastic simulation of daily climate data. U. S. Dept. Agric., Stat. Rep. Serv., Res. Div. SRS Staff Rep No. AGES810831.
Lee, D. M. (1979). Australian drought watch system. In *Proceedings of the Symposium on Drought in Botswana*, ed. M. T. Hinchey, 173–207. Hanover, NH, University Press of New England.
Little, M. A., N. Dyson-Hudson, R. Dyson-Hudson, J. E. Ellis and D. M. Swift. (1984). Human biology and the development of an ecosystem approach. In *The ecosystem concept in anthropology*, ed. E. Moran, 103–31. Boulder, CO, Westview Press.
Mason, J. B., J. G. Haaga, T. O. Maribe, G. Marks, V. J. Quinn and K. E. Test. (1987). Using agricultural data for timely warning to prevent the effects of drought on child nutrition on Botswana. *Ecol. Food and Nutrition*, **19**, 169–84.
McCabe, J. T. (1983). Land use among the pastoral Turkana. *Rural Africana*, **15–16**, 109–126.
McCabe, J. T. (1987). Variation in livestock production and its impact on social organization. *J. Res. Econ. Anthrop.*, **8**, 277–93.
McCabe, J. T. and J. E. Ellis. (1987). Beating the odds in arid Africa. *Natural History*, **96**(1), 33–41.
Milford, J. R. (1987). Problems for deducing the soil water balance in dryland regions from Meteosat data. *Soil Use and Manage.*, **3**, 51–6.
Morgan, R. (1985). The development and applications of a drought early warning system in Botswana. *Disasters*, **9**, 44–50.
Pickup, G. and V. H. Chewings. (1988). Estimating the distribution of grazing and patterns of cattle movement on a large arid zone paddock. *Int. J. Rem. Sens.*, **9**, 1469–90.
Prince, S. D. and C. J. Tucker. (1986). Satellite remote sensing of rangelands in Botswana II. NOAA AVHRR and herbaceous vegetation. *Int. J. Rem. Sens.*, **7**, 1555–70.
Swift, D. M. (1987). Structure of the drought simulation model. In Pastoralism and drought in Turkana District Kenya, ed. J. E. Ellis, K. A. Galvin, J. T. McCabe and D. M. Swift. A report to the Norwegian Agency for International Development (NORAD), Nairobi, Kenya.
Swift, J. (1985). Planning against drought and famine in Turkana, Northern Kenya. Oxfam and Turkana Rehabilitation Project, Nairobi, Kenya.
Tucker, C. J., C. VanPraet, E. Boerwinkel and A. Gaston. (1983). Satellite remote sensing of total dry matter production in the Senegalese Sahel. *Rem. Sens. Env.*, **13**, 461–74.
Tucker, D. J., J. R. Townsend and T. E. Goff. (1985). African land-cover classification using satellite data. *Science*, **227**, 369–75.

Verstappen, H. Th. (1979). Drought susceptibility survey and the concept of monitoring landscape ecology. In *Proceedings of the Symposium on Drought in Botswana*, ed. M. T. Hinchey, 75–81. Hanover, NH, University Press of New England.
Waring, R. H., J. D. Aber, J. M. Melillo and B. Moore. (1986). Precursors of change in terrestrial ecosystems. *Bioscience*, **36**, 433–8.

SI

Environmental Co
Dr. Erich W. Bre
Office of Researcl
US EPA (RD 67
401 M. St., SW
Washington, DC
USA

Dr. Daniel H. M
US EPA
200 SW 35th St.
Corvallis, OR 97
USA

Ecological Indicat
Professor Dr. Sver
Dept. of Environn
Royal Danish Sch
2 Universitet Spa
Copenhagen DK-
Denmark